J. Membrane Biol. 81, 49–58 (1984)

The Journal of
Membrane Biology

Communicating Junctions and Calmodulin: Inhibition of Electrical Uncoupling in *Xenopus* Embryo by Calmidazolium

Camillo Peracchia
Department of Physiology, University of Rochester, Rochester, NY 14642

Summary. This paper reports the inhibitory effects of calmidazolium (CDZ), a calmodulin inhibitor, on electrical uncoupling by CO_2. Membrane potential and coupling ratio (V_2/V_1) are measured in two neighboring cells of *Xenopus* embryos (16 to 64 cell stage) for periods as long as 5.5 hr. Upon exposure to 100% CO_2, control cells consistently uncouple even if the CO_2 treatments are repeated every 15 min for 2.5 hr. CDZ ($5 \times 10^{-8} - 1 \times 10^{-7}$ M) strongly inhibits uncoupling. The inhibition starts after 30, 50 and 60 min of treatment with 1×10^{-7}, 7×10^{-8} and 5×10^{-8} M CDZ, respectively, is concentration-dependent and partially reversible. In the absence of CO_2, CDZ also improves electrical coupling. CDZ has no significant effect on membrane potential and nonjunctional membrane resistance. These data suggest that calmodulin or a calmodulin-like protein participates in the uncoupling mechanism.

Key Words electrical coupling · uncoupling · calmodulin · cell-to-cell channels · gap junctions · *Xenopus* embryos

Introduction

A form of direct cell-to-cell communication is believed to be mediated by cell-to-cell channels located in gap junctions, the coupling junctions. These channels can be closed by a variety of treatments known to modify the intracellular ionic composition (reviewed in Peracchia, 1980, 1984). A large body of evidence indicates that channel occlusion (cell uncoupling) is induced by divalent cations, primarily Ca^{++} (Loewenstein, 1981), but recently intracellular acidification has also been found to cause cell uncoupling, suggesting that H^+ may also affect channel permeability (Turin & Warner, 1977, 1980; Spray, Harris & Bennett, 1981*a*; Spray, Stern, Harris & Bennett, 1982).

In spite of our knowledge of uncoupling agents, little is known about the uncoupling mechanism. We have proposed that uncoupling may result from a conformational change in the channel proteins induced by activated calmodulin (Peracchia, Bernardini & Peracchia, 1981, 1983). This has been formulated on the basis of morphological and electrophysiological data obtained with a calmodulin inhibitor, trifluoperazine hydrochloride (TFP) (Weiss, Fertel, Figlin & Uzonov, 1974). TFP was found to prevent the Ca^{++} and H^+-induced ordering of lens gap junction particles, previously shown in other tissues to occur associated with electrical cell-to-cell uncoupling (Peracchia, 1982*a*), and to strongly inhibit the CO_2-induced electrical uncoupling of *Xenopus* embryonic cells (Peracchia et al., 1981, 1983). The possible calmodulin involvement in gap junction function has also been supported by the observation that calmodulin binds specifically to the lens and liver gap junction proteins (Welsh et al., 1981, 1982; Hertzberg & Gilula, 1981).

Van Belle (1981) has developed a calmodulin inhibitor more powerful and specific than TFP: calmidazolium (R 24571). The present study reports electrophysiological data demonstrating the inhibitory effects of calmidazolium on electrical uncoupling of *Xenopus* embryonic cells, supporting the involvement of calmodulin in the regulation of cell coupling. A preliminary account of this study has been published (Peracchia, 1982*b*).

Materials and Methods

Experimental Preparation

Xenopus laevis embryos were used at the16–64 cell stage. The jelly surrounding the embryos was carefully removed with two fine forceps, and the embryos were placed on the bottom of a saline-filled plexiglass chamber coated with Sylgard 184 resin. The preparations were continuously superfused at room temperature (~20°C) with saline solutions flowing at a rate of 2 ml/min. Both a modified Holtfreter's and a modified amphibian Ringer's solution were used. The composition of the Holtfreter's solution was (in mM): NaCl, 60; KCl, 0.67; $CaCl_2$, 0.9; $NaHCO_3$, 10. That of the Ringer's solution was (in mM): NaCl, 111; KCl, 1.9; $CaCl_2$, 1.32; $NaHCO_3$, 12. Before use, the saline solutions were bubbled with 95% O_2, 5% CO_2, to a final pH of 7.2.

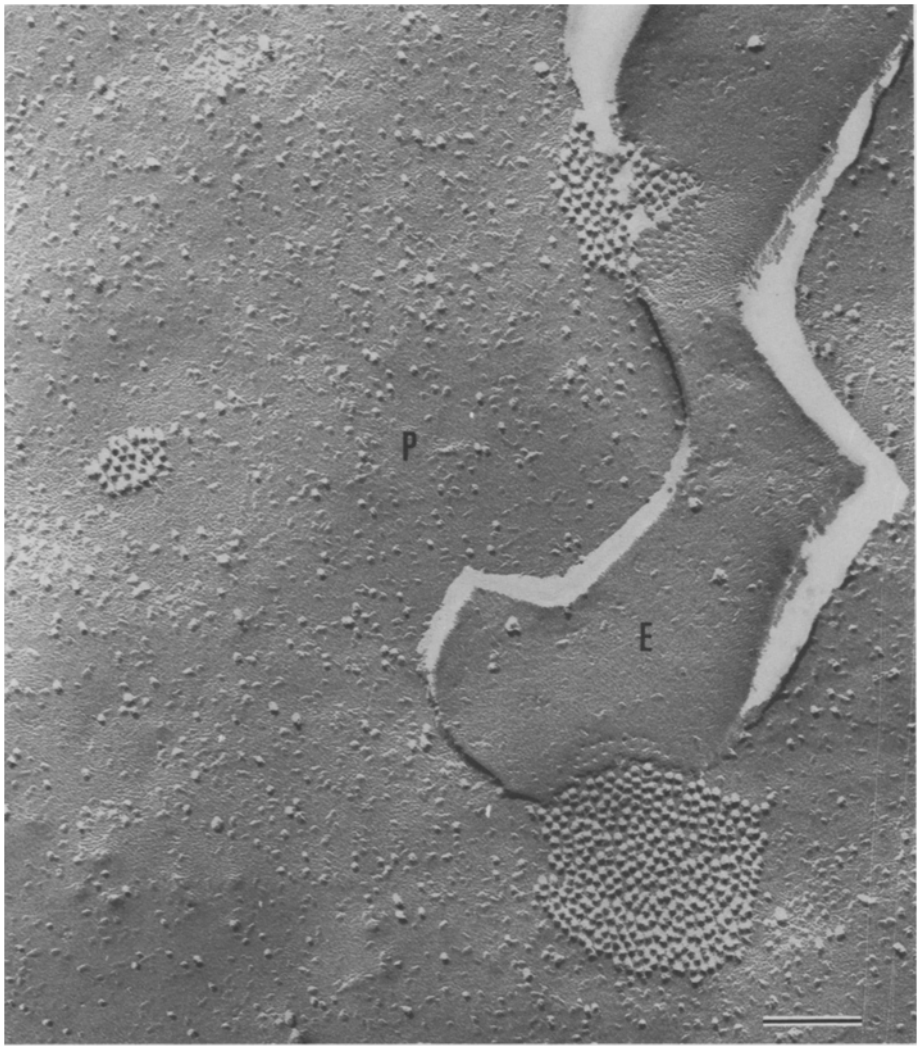

Fig. 1. Freeze-fracture replica of control *Xenopus* embryo cells at a preblastula stage of development. The protoplasmic face (*P*) and the exoplasmic face (*E*) of two neighboring cell membranes display randomly distributed particles and pits as well as three small gap junctions. The two junctions on the right show particles on the *P* face and a few complementary pits on the *E* face, that on the left only particles. The disordered particle packing and the center-to-center particle spacing (~10 nm) are typical of vertebrate gap junctions fixed in a coupled state (Peracchia, 1980). Bar = 0.1 μm

Calmidazolium-saline solutions were prepared by adding a concentrated solution of 1-[bis(*p*-chlorophenyl)methyl]-3-[2,4-dichloro-β-(2,4 dichlorobenzyloxy) phenetyl] imidazolium chloride, calmidazolium (CDZ) (R 24571, Janssen Pharmaceutica, Beerse, Belgium) (Van Belle, 1981) to the saline solutions, to reach final CDZ concentrations of 1×10^{-7}, 7×10^{-8} and 5×10^{-8} M. CDZ stock solutions, either in H_2O (4.8×10^{-5} M) or in DMSO (5×10^{-3} M), were stored at 4°C not longer than 4 weeks.

To cause cell-to-cell electrical uncoupling, the perfusing saline or CDZ saline solutions were bubbled with 100% CO_2. CO_2 bubbling lowered the pH of the saline solution to 5.8–5.9. CDZ (10^{-7} M) did not affect the pH of the solutions and the pH changes caused by CO_2. When solutions were changed, the new solution reached a constant concentration in the bath in less than 2 min. This was determined by measuring the fluorescence emission of a procion yellow solution sampled in the bath at 30-sec intervals.

Electrophysiology

Microelectrodes, pulled from 1.2 mm (OD) glass capillaries with a vertical puller (D. Kopf Instruments, Tujunga, CA), were filled with a filtered 3 M KCl and 15 mM K-citrate solution. Two microelectrodes with a final resistance of 5–15 MΩ were inserted into neighboring cells of a *Xenopus* embryo epi-illuminated with a fiber optic illuminator (Fiber-lite 180, Dolan-Jenner, Woburn, MA) and viewed with a Wild M4A stereomicroscope at 60× magnification.

One microelectrode, connected to a WPI 701 M microprobe amplifier (W-P Instruments, Inc., New Haven, CT), injected current and measured membrane potential (E_1) and electrotonic potential (V_1) in cell one (C_1). The other microelectrode, connected to a WPI 725 micro-probe amplifier, measured membrane potential (E_2) and electrotonic potential (V_2) in cell two (C_2). The bath was grounded via an Ag/AgCl electrode.

Stimulus pulses were produced by a WPI stimulus isolator module (1850-A) coupled with a WPI digital pulse generator system. Voltage pulses were converted to constant current pulses by the 701 M amplifier. Hyperpolarizing rectangular current pulses (5 nA, 300 msec duration) were injected at 10-sec intervals. The resulting V_1 and V_2 were displayed on a storage oscilloscope (5113, Tektronix, Beaverton, OR) and on a pen recorder (2200, Gould, Cleveland, OH). Each V_1 displayed on the oscilloscope was checked for balance. Bridge unbalance was recognized as a fast rising step in voltage preceding the slower voltage

component associated with the membrane. In case of unbalance, the 701 M amplifier was quickly readjusted by eliminating the fast rising step in voltage.

In all the experiments, the two microelectrodes were kept in the same two neighboring cells throughout the experiment. The capacity of the cells to uncouple with CO_2 was tested several times in control salines before superfusing the embryos with CDZ-saline solutions as these cells begin to uncouple consistently with CO_2 only from the 16-cell stage on (Turin & Warner, 1980; G. Bernardini & C. Peracchia, *unpublished observation*).

For measuring the effects of CDZ on the membrane resistance of individual embryonic cells, 16–64 cell embryos were dissociated into individual cells by cutting them open, after mechanical removal of the jelly, and shaking them in the Ringer's solution of the plexiglass chamber. This method results in the dissociation of many healthy cells. For single cell recording, a microelectrode was inserted in 50–80 μm cells. Hyperpolarizing current pulses of 100–200 pA were injected and the resulting potentials were recorded through the same microelectrode as described above. The input resistance was calculated both before and during exposure to 100% CO_2 in the presence and absence of 1×10^{-7} M CDZ. The measurements were performed after CDZ treatments 30 to 300 min long. The input resistance was measured in each cell every 50 sec, and both its mean and standard error values from several cells were calculated.

Electron Microscopy

Xenopus embryos, fixed overnight at room temperature with a 3% glutaraldehyde solution buffered to pH 7.4 with 0.1 M Na-cacodylate, were freeze-fractured with a Balzers BAF 301 freeze-etch unit (Balzers High Vacuum Corp., Santa Ana, CA), as previously described (Peracchia & Peracchia, 1980). The replicas were viewed and photographed with an AEI EM 801 electron microscope.

Results

Junction Ultrastructure

Gap junctions and spot desmosomes are the only junctions connecting neighboring cells of *Xenopus* embryos at early stages of development. At the blastula stage, also tight junctions appear, both as maculae and zonulae occludentes. The gap junctions (Fig. 1) are scarce and tend to be aggregated into 5–10 μm^2 areas. They range from 0.05 to 3 μm in diameter, the majority being ~0.1 μm, and display structural features typical of vertebrate gap junctions (Peracchia, 1980), with particles loosely packed at a center-to-center spacing of ~10 nm.

Electrical Coupling and Uncoupling

Xenopus embryo cells from the two-cell stage on have a membrane potential of −30 to −60 mV and are electrically well coupled. Hyperpolarizing current pulses of 5 nA injected into C_1 result in V_1 of 3–5 mV and slightly smaller V_2. The coupling coefficient (V_2/V_1) is 0.6–1 in cells superfused with Holtfreter's solution (Figs. 2 and 5*D*) and 0.4–0.6 in cells superfused with Ringer's solution (Figs. 3*D* and 6*B*). Upon superfusion with either saline bubbled with 100% CO_2 (Figs. 3*A*, 5*A* and 6*A*), at first both cells become slightly hyperpolarized (3–5 mV) for approximately 1 min and then depolarize, E_1 and E_2 reaching values of −5 to −10 mV. V_1 increases and V_2 decreases, causing the coupling coefficient (V_2/V_1) to progressively decrease, starting 1–2 min after the beginning of CO_2 treatment, down to values of 0.01 to 0.05 within 5–7 min of CO_2 treatment (Figs. 2, 3*D*, 5*D* and 6*B*). Upon return to normal saline, E_1, E_2 and V_2/V_1 rapidly return to control values, the recovery process taking 5–10 min (Figs. 3*A*, 5*A* and 6*A*).

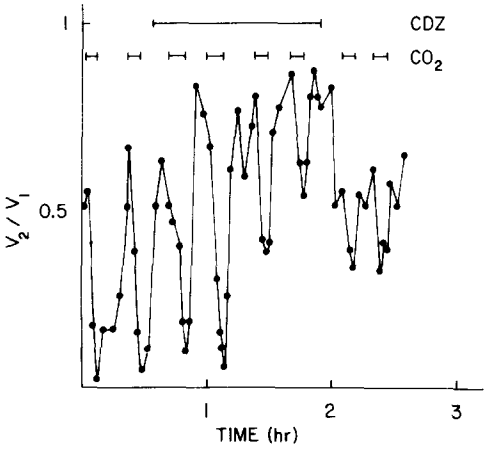

Fig. 2. Effects of 1×10^{-7} M calmidazolium (CDZ) in Holtfreter on CO_2-induced electrical uncoupling of two adjacent cells of a *Xenopus* embryo. Time course of the coupling ratio (V_2/V_1) was sampled from a continuous chart recording. The bars represent the periods of exposure to 100% CO_2 and CDZ. Before CDZ treatment a 5-min exposure to CO_2 causes uncoupling, resulting in V_2/V_1 as low as 0.025. Uncoupling inhibition starts after approximately 30 min of CDZ treatment and proceeds fairly rapidly, such that after 72 min of CDZ treatment a 6-min exposure to CO_2 does not lower V_2/V_1 below 0.53. Upon removal of CDZ there is a partial recovery of the uncoupling mechanism. Notice that CDZ also reversibly increases the coupling ratio (V_2/V_1) in the absence of CO_2

Inhibition of Electrical Uncoupling by Calmidazolium (CDZ)

Superfusing *Xenopus* embryos with either saline containing 5×10^{-8} to 1×10^{-7} M CDZ, for periods as long as 4 hr strongly inhibits electrical uncoupling by 100% CO_2 without affecting membrane po-

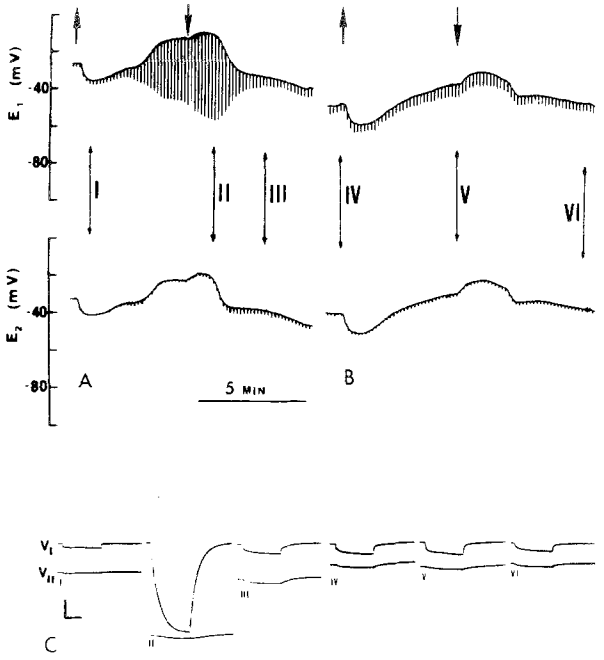

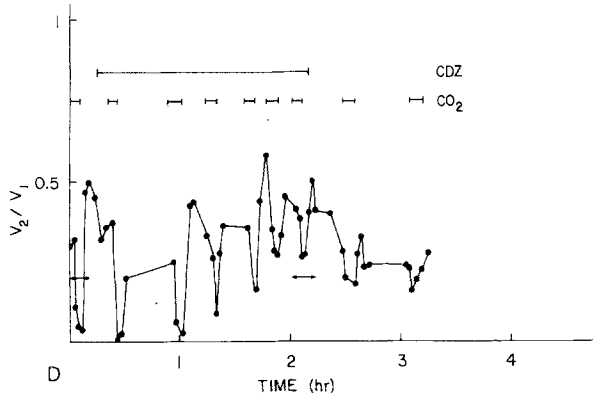

Fig. 3. Effects of 7×10^{-8} M calmidazolium (CDZ) in Ringer on CO_2-induced electrical uncoupling of two adjacent cells of a *Xenopus* embryo. *A* and *B* show low speed chart recordings of membrane (E_1, E_2) and electrotonic (V_1, V_2) potentials in cell one (C_1) and two (C_2), respectively, during the periods indicated in *D* by the double-headed arrows (left without CDZ and right with CDZ). The large arrows mark beginning (↑) and end (↓) of exposures to 100% CO_2, and the double-headed arrows labeled with Roman numerals refer to the corresponding oscilloscope recordings (V_1 and V_2) shown in *C*. *D* shows the time course of the coupling ratio (V_2/V_1) sampled from the continuous chart recording shown in part in *A* and *B*. The bars represent the periods of exposure to 100% CO_2 and CDZ. CDZ inhibition of CO_2 uncoupling starts 50 min after the beginning of the treatment and proceeds fairly linearly at a slower rate than with 1×10^{-7} M CDZ (Fig. 2). After 112 min of CDZ treatment, V_2/V_1 does not decrease below 0.26 with a 6-min exposure to CO_2 (*B*, *C* (*V*) and *D*), while before CDZ treatment the same cells reach a V_2/V_1 of 0.01 with a 5-min exposure to CO_2 (*A*, *C*(*II*), and *D*). Note the partial recovery of the uncoupling mechanism after removal of CDZ (*D*). In *C*, vertical bar = 10 mV; horizontal bar = 150 msec

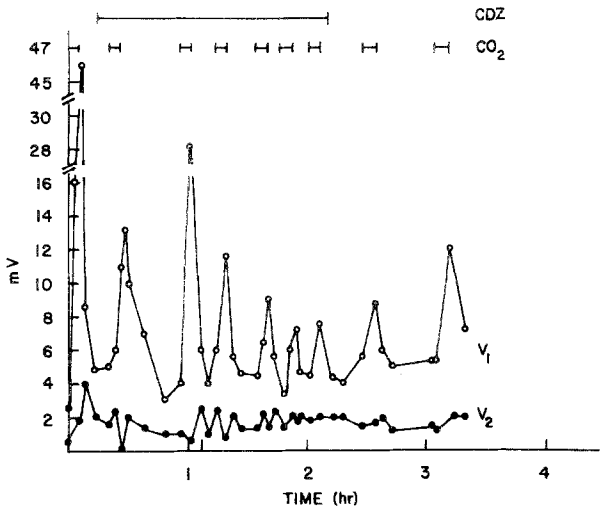

Fig. 4. Time course of V_1 and V_2 amplitudes from the experiment shown in Fig. 3. Note the lack of significant changes in V_1 and V_2 amplitudes (in the intervals between CO_2 exposures) during the CDZ treatment. This indicates that the CDZ treatment does not significantly affect input and transfer resistances

tential and input resistance. The onset as well as the rate of uncoupling inhibition are dose-dependent (Fig. 7). The inhibition starts after approximately 30, 50 and 60 min of treatment with 1×10^{-7} M (Fig. 2), 7×10^{-8} M (Fig. 3*D*) and 5×10^{-8} M (Fig. 5*D*) CDZ, respectively; approximately at the same time the cells stop dividing. The uncoupling inhibition progresses fairly linearly, at a dose-dependent rate, for at least 1 hr (Fig. 7). In cells exposed to a low CDZ concentration, an increase in CDZ concentration causes a rapid increase in the rate of uncoupling inhibition (Fig. 5*D*).

The greatest uncoupling inhibition is obtained with 1×10^{-7} M CDZ (Fig. 2), but even 5×10^{-8} M CDZ (Fig. 5) is effective. In CDZ-treated cells, longer exposures to CO_2 (up to 15 min) do not significantly lower the V_2/V_1 values below those reached after the usual 5–6 min of CO_2 exposure.

Throughout the length of a CDZ treatment the amplitudes of V_1 and V_2, in the absence of CO_2, do not vary significantly and are similar to those of the control and recovery periods, indicating the lack of a sizable change in input resistance. This is clearly seen in Fig. 4, where the potentials (V_1 and V_2) of the experiment shown in Fig. 3, are individually plotted against time.

Upon CDZ washout, the cells partially recover their ability to uncouple with CO_2 (Figs. 2, 3*D*, 5*D* and 7) even after CDZ treatments longer than 4 hr (Fig. 5*D*), but whether or not a complete recovery of the uncoupling mechanism can be achieved, was not determined. In many experiments CDZ also im-

proved coupling. A sizeable increase in V_2/V_1 in the absence of CO_2 (Figs. 2 and 6*B*) was observed in six experiments; in one experiment V_2/V_1 increased only after the CDZ concentration was increased from 5×10^{-8} to 1×10^{-7} M (Fig. 5); only in one experiment was there no change in V_2/V_1 with 10^{-7} M CDZ. The increase in V_2/V_1, in the absence of CO_2, obviously has to be considered in evaluating the effects of CDZ on uncoupling. In Fig. 2, for example, since V_2/V_1 in the absence of CO_2 is greater during CDZ treatment than during the control period, the increase in the minimum V_2/V_1 in CO_2, during CDZ exposure, is less significant in terms of improved junctional conductance than one would expect if only the V_2/V_1 minima were considered. However, in spite of this, the CDZ-induced uncoupling inhibition is obvious in all the experiments. For example, in Fig. 5 the starting V_2/V_1's in CDZ are similar or smaller than those recorded in the absence of CDZ, yet the V_2/V_1's drop less with CO_2 than before the CDZ treatment. In the absence of CDZ the cells are able to uncouple repeatedly and effectively, with CO_2, for several hours, even if the CO_2 treatments are repeated every 15–20 min (Figs. 6 and 7).

CDZ does not significantly affect the nonjunctional membrane resistance. In individual embryonic cells isolated from 16–64 cell embryos and treated with 1×10^{-7} M CDZ, the membrane resistance, in the absence of CO_2, and its increase during CO_2 exposure are not significantly different from those of control cells. This is seen in Fig. 8, which plots mean and standard error values of the membrane resistances calculated from 14 cells treated with 1×10^{-7} M CDZ for periods ranging from 30 to 300 min (Table) and from 11 control cells.

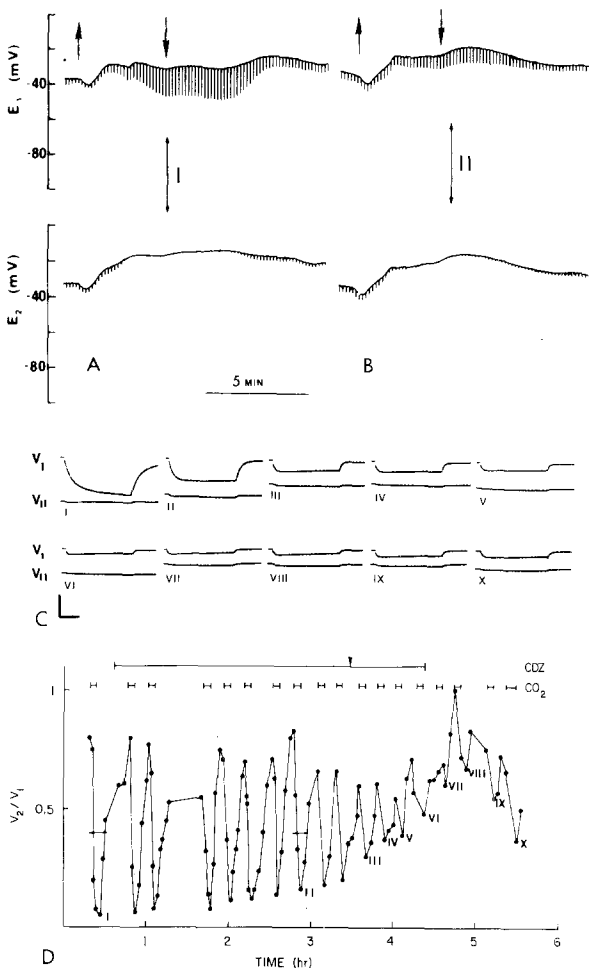

Fig. 5. Effects of 5×10^{-8} and 1×10^{-7} M calmidazolium (CDZ) in Holtfreter on CO_2-induced electrical uncoupling of two adjacent cells of *Xenopus* embryo. Labeling is as indicated in Fig. 3. The location of the oscilloscope potentials shown in *C* is indicated in *D* (with Roman numerals); that of the *I* and *II* potential is also indicated in *A* and *B*, respectively. With 5×10^{-8} M CDZ the inhibition of CO_2 uncoupling starts 60 min after the beginning of the treatment and proceeds fairly linearly at a slow rate (*D*). After 137 min of treatment with 5×10^{-8} M CDZ, V_2/V_1 does not decrease below 0.2, with a 5-min CO_2 exposure [*B*, *C(II)*, and *D(II)*], while without CDZ the same cells reach a V_2/V_1 of 0.025 with a similar CO_2 treatment [*A*, *C(I)*, and *D(I)*]. Upon increase to 1×10^{-7} M CDZ (*D*, arrowhead), the rate of inhibition increases sharply such that in 55 min V_2/V_1 decreases with CO_2 only to 0.48 [*C(VI)* and *D(VI)*]. After CDZ removal, the inhibition continues for approximately 30 min, resulting in V_2/V_1 with CO_2 as high as 0.67 [*C(VIII)* and *D(VIII)*], then decreases sharply such that 67 min after CDZ removal a CO_2 exposure lowers V_2/V_1 to 0.36 [*C(X)* and *D(X)*]. In *C*, vertical bar = 10 mV, horizontal bar = 100 msec

Discussion

This study shows that a specific calmodulin blocker, calmidazolium (CDZ) reversibly inhibits the CO_2-induced cell-to-cell electrical uncoupling of *Xenopus* embryos at the 16–64 cell stage, without significantly affecting the membrane potential and the input resistance of these cells. CDZ may prevent the occlusion of the cell-to-cell channels of gap junctions, which together with rare desmosomes are the only junctions connecting the cells of *Xenopus* embryos at this early stage of development.

The inhibitory effect of CDZ begins after a dose-dependent delay. A reason for the delay could be the slow diffusion of CDZ across the plasma membrane. CDZ, an analogue of sepazonium, is a lipophilic compound and thus is expected to enter the cells by diffusing through the lipid bilayer. However, its size (mol wt = 688) and positive charge may slow the diffusion process and its lipophilicity may cause it to distribute evenly among the various lipid compartments of the cell, keeping low for

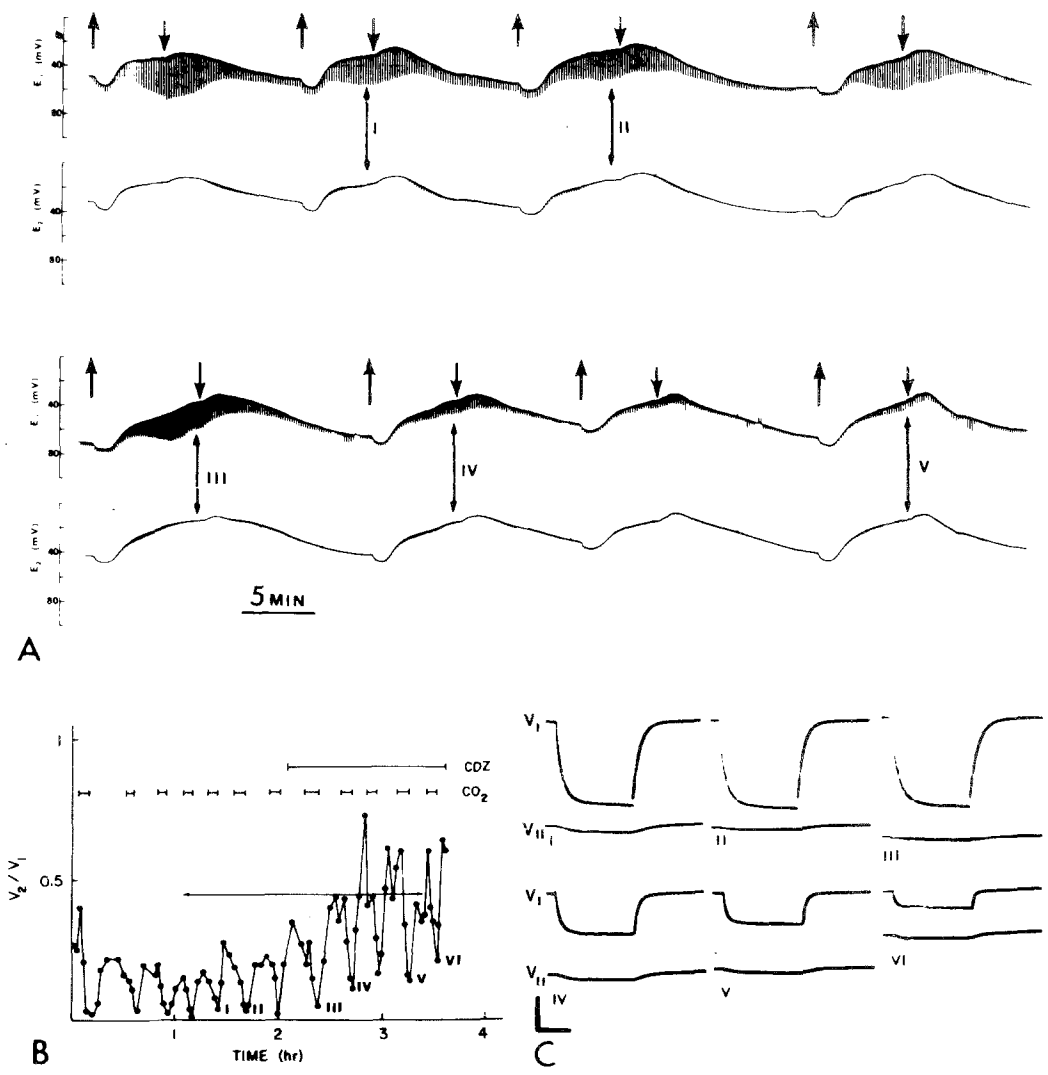

Fig. 6. Effects of repeated CO_2 treatments on electrical coupling between *Xenopus* embryo cells (Ringer). Labeling is as indicated in Fig. 3. The location of the oscilloscope potentials *I* to *V* shown in *C* is indicated with Roman numerals in *A* and *B*; that of the *VI* potentials is only indicated in *B*. Note that CO_2 treatments repeated for over 2 hr in the absence of CDZ cause similar uncoupling effects (*B*), as V_2/V_1 decreases consistently to values of 0.01–0.04. Upon treatment with 1×10^{-7} M CDZ, uncoupling inhibition gradually develops (*B*), as subsequent CO_2 exposures are progressively less effective in lowering the coupling ratio (V_2/V_1). In *C*, vertical bar = 10 mV; horizontal bar = 150 msec

some time its cytoplasmic concentration. That CDZ enters the cells is suggested by the fact that cell division stops approximately when the uncoupling inhibition starts. Indeed, there is evidence that calmodulin is involved in microtubule function during mitosis (Welsh, Dedman, Brinkley & Means, 1978, 1979) and that CDZ inhibits the Ca^{++}-induced microtubule polymerization (Schliwa, Euteneuer, Bulinski & Izant, 1981).

The inhibition of uncoupling is not the result of an exhaustion of the uncoupling mechanism because in the absence of CDZ the cells are able to uncouple repeatedly for several hours, with a similar time course, and because the CDZ inhibition is dose dependent and is partially reversible. The CDZ-induced improvement of electrical coupling, in the absence of CO_2, indicates that some of the intercellular channels may be closed even in control conditions. A CDZ inhibition of the occluding mechanism would result in an increase in the fraction of open channels at any given time, thus improve coupling. Alternatively, CDZ could increase the conductance of the open channels or increase the total number of available channels.

The effects of CDZ are not the result of changes in the electrical properties of the nonjunctional

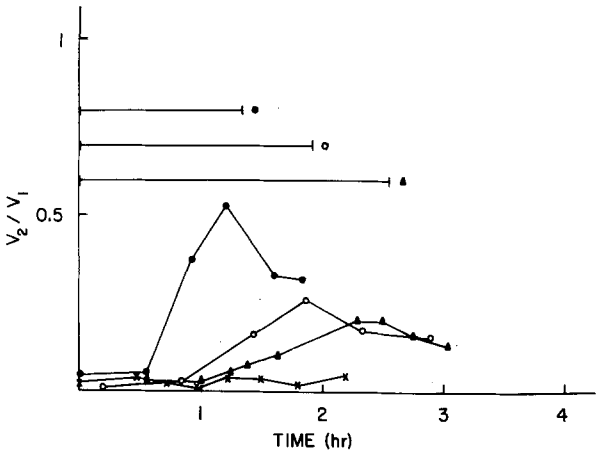

Fig. 7. Time course of minimum coupling ratios (V_2/V_1) measured between neighboring *Xenopus* embryo cells upon exposures to 100% CO_2 in the presence of 1×10^{-7} M (filled circles), 7×10^{-8} M (open circles), 5×10^{-8} M (triangles) CDZ and in the absence of CDZ (x's)

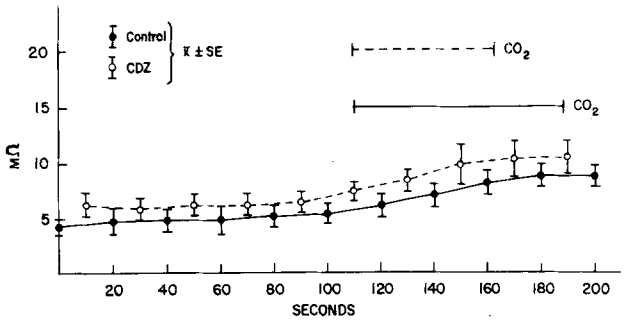

Fig. 8. Time course of the membrane resistances of individual cells (50–80 μm in diameter), isolated from 16–64 cell *Xenopus* embryos, in control conditions (filled circles) and after treatment with 1×10^{-7} M CDZ for periods of 30–300 min (open circles), before and after exposure to 100% CO_2. The points on the curves are means ± SE values of input resistance calculated from 11 control cells and 14 CDZ-treated cells. The cells were injected with hyperpolarizing current pulses of 100–200 pA

Table.

CDZ (10^{-7} M) exposure time (in minutes)	Input resistance in MΩ (mean ±SE)	
	Before CO_2 effect (0–100 sec)	After CO_2 effect (100–200 sec)
30–60 (5 cells)	8.16 ± 2.04	10.78 ± 3.04
60–180 (7 cells)	4.9 ± 0.64	8.84 ± 2.44
180–300 (2 cells)	5.25 ± 0.79	11.3 ± 3.89

Mean ±SE values of input resistance in individual cells isolated from 16–64 cell *Xenopus* embryos (before and after CO_2 exposure) and treated for different lengths of time with 1×10^{-7} M CDZ, in the presence and absence of 100% CO_2. Note that even CDZ treatments of 3 to 5 hr have little effect on membrane resistance.

membrane as significant changes in membrane potential and input resistance were not detected. While a direct measurement of membrane resistance in the intact embryos could not be performed, the lack of significant changes in the membrane resistance of isolated embryonic cells, both in the presence and absence of CO_2, after long exposures to CDZ clearly indicates that this drug has a minimal, if any, effect on the nonjunctional membrane resistance. This is also supported by the fairly constant values of input and transfer resistance in the cells of intact embryos. Indeed, only a very large, two to three orders of magnitude, increase in nonjunctional membrane resistance could account for an increase in V_2/V_1, in the presence of 100% CO_2, from 0.025 (control) to 0.53 (CDZ) (Fig. 2) (Socolar & Loewenstein, 1979).

The uncoupling inhibition is likely to result from calmodulin inhibition because the CDZ concentrations effective on uncoupling are similar to those that specifically inhibit calmodulin. In fact, the I_{50} (50% inhibition) of various calmodulin-activated enzymes is given by CDZ concentrations in the 10^{-8}–10^{-7} M range and these doses do not affect various dopaminergic and serotonergic receptors (Van Belle, 1981) which are affected by I_{50}-doses of other calmodulin blockers (phenothiazines) (Backmore et al., 1981).

However, the possibility that CDZ inhibits uncoupling via a mechanism not involving calmodulin cannot be discarded. An apparent uncoupling inhibition could result from an increase in the paracellular resistance (between the blastocoele and the bath). Indeed, a reduction in the effects of CO_2 would occur if CDZ were causing a decrease in tight-junction permeability as this would result in a more effective current flow from cell to cell through the intercellular spaces. However, this is unlikely because in our freeze-fracture replicas tight junctions were seen only at later stages of embryonic development, the only junctions present up to the 64-cell stage being gap junctions and spot desmosomes. In any event, there is no evidence that CDZ has any effects on tight-junction function and/or on paracellular resistance.

A calmodulin involvement in coupling regulation would not be surprising, as a vast literature reports the close relationship between an increase

in cytoplasmic-free calcium and electrical uncoupling (reviewed in Loewenstein, 1981). However, the present study and previous findings on the inhibition of CO_2 uncoupling by trifluoperazine hydrochloride (Peracchia et al., 1981, 1983) raise a number of questions. Uncoupling by CO_2 is believed to be a consequence of cytoplasmic acidification and, possibly, to be the result of a direct action of H^+ on the channel proteins (Turin & Warner 1977, 1980; Rink, Tsien & Warner, 1980; Spray et al., 1981*a*). A possible interpretation is that the CO_2-induced uncoupling is also a Ca^{++} mediated phenomenon (Rose & Rick, 1978). Indeed, recently fine changes in the structure of isolated gap junctions have been detected by X-ray diffraction with increased [Ca^{++}] but not with decreased pH (Unwin & Ennis, 1983). However, the relationship between these changes and the channel function is still hypothetical. Alternatively, calmodulin could be affected by H^+, as it is by Ca^{++} and other divalent cations. Calmodulin crystallizes at pH 6 as well as in Ca^{++} media (Kretsinger, 1980), and each of its Ca^{++} sites contains several carboxyl groups with a high pK_a. Indeed, in troponin C, a molecule structurally and functionally similar to calmodulin, the carboxyl groups of the Ca^{++} sites have a pK_a of 6.0 and their protonation induces conformational and tyrosyl fluorescence changes (starting at pH 6.5) similar to those caused by Ca^{++} (Lehrer & Leavis, 1974). Recently, similar data have been obtained with calmodulin (Steiner, Lamboy & Sternberg, 1983). This study, using such criteria as tyrosine ϕ_{em} relaxation time, circular dichroism, and viscosity, showed that calmodulin in lovered pH mimics in conformation its Ca-activated form. However, the independent effect of H^+ on calmodulin activity is yet to be tested.

The mechanism by which calmodulin activation may affect channel permeability is not known. The channel protein could be calmodulin receptors and undergo conformational changes upon interaction with activated calmodulin. Alternatively, calmodulin could activate an enzymatic machinery, affecting the channel protein indirectly. In view of the well-known calmodulin involvement in both the synthesis and the breakdown of cAMP, calmodulin inhibition could affect coupling via a change in cAMP concentrations. Indeed, an increase in cAMP has been shown to improve coupling in various cultured cells (Azarnia, Dahl & Loewenstein, 1981; Flagg-Newton, Dahl & Loewenstein, 1981; Flagg-Newton & Loewenstein, 1981) and in rat heart (Estapé-Wainwright & DeMello, 1983), while it caused uncoupling in the horizontal cells of the retina (Teranishi, Negishi & Kato, 1983) and it accelerated uncoupling in cat heart (Wojtczak, 1982). Calmodulin inhibition could interfere with phosphorylation of the channel protein or associated proteins, as calmodulin activates a number of kinases. Recently, the function of a variety of membrane channels has been proposed to be modulated by cAMP and phosphorylation (Siegelbaum, Camardo & Kandel, 1983; Green & Gillette, 1983; Bean, Nowycky & Tsien, 1983).

Recent data, however, may support a more direct calmodulin involvement in channel function. In lens junctions, calmodulin has been shown to bind directly and in a Ca^{++}-independent manner to the junction protein (MIP 26) (Welsh et al., 1981, 1982; Hertzberg & Gilula, 1981) and similar results have been obtained with the liver gap-junction protein, but here the binding was Ca^{++} dependent (Hertzberg & Gilula, 1981). The intrinsic tryptophan fluorescence of isolated MIP 26 decreases by 20% in the presence of Ca^{++}-activated calmodulin, indicating conformational changes in the junction protein (Girsch & Peracchia, 1982). These data have been confirmed in circular dichroism experiments in which Ca^{++}-activated calmodulin was found to increase the helical content of MIP 26 (Girsch & Peracchia, 1983*a*). In addition, preliminary experiments indicate that the permeability of large channels formed by the incorporation of lens gap-junction protein (MIP 26) into liposomes is reversibly regulated by Ca-calmodulin (Girsch & Peracchia, 1983*b*).

A calmodulin involvement in cell coupling has also been suggested in insect epidermis (Lees-Miller & Caveney, 1982). In this system calmodulin inhibitors induced rather than inhibited uncoupling. However, the concentrations at which they induced uncoupling were much greater (5–100 times) than those known to specifically inhibit calmodulin. Moreover, the calmodulin inhibitors consistently caused a drastic membrane depolarization in parallel with uncoupling. In this study, whether or not the uncoupling was the result of calmodulin inhibition rather than depolarization was not convincingly proven. Indeed, recently Obaid, Socolar and Rose (1983) have shown that depolarization itself can cause uncoupling in another insect epithelium (*Chironomus* salivary gland cells). There are reasons to believe that pH and voltage sensitivity of channel conductance belong to different regulatory sites (Spray, Harris & Bennett, 1981*b*).

In conclusion, this study shows that CDZ, a specific calmodulin blocker, strongly inhibits electrical uncoupling by 100% CO_2 and improves coupling in *Xenopus* embryo cells. These data confirm and extend previous findings on the inhibitory effects of another calmodulin blocker, trifluoperazine hydrochloride, on electrical uncoupling in amphibian embryos (Peracchia et al., 1981, 1983) and sug-

gest that direct cell-to-cell communication may be regulated by calmodulin or a calmodulin-like protein.

I am indebted to Drs. Mei-Ven C. Lo, Peter Shrager, and Todd Scheuer for their helpful discussion and criticism, to Dr. Stephen J. Girsch for performing the fluorescence measurements, and to Lillian L. Peracchia for excellent technical assistance.

This work was supported by NIH grant GM 20113.

References

Azarnia, R., Dahl, G., Loewenstein, W.R. 1981. Cell junction and cyclic AMP: III. Promotion of junctional membrane permeability and junctional membrane particles in a junction-deficient cell-type. *J. Membrane Biol.* **63:**133–146

Bean, B.P., Nowycky, M.C., Tsien, R.W. 1983. β-Adrenergic modulation of calcium channels in frog ventricular heart cells. *Nature (London)* **307:**371–375

Blackmore, P.F., El-Rafai, M.F., Dehaye, J.-P., Strickland, W.G., Hughes, B.P., Eaton, J.H. 1981. Blockade of hepatic α-adrenergic receptors and responses by chlorpromazine and trifluoperazine. *FEBS Lett.* **123:**245–248

Estapé-Wainwright, E., DeMello, W.C. 1983. Cyclic nucleotides and calcium: Their role in the control of cell communication in the heart. *Cell Biol. Int. Rep.* **7:**91–97

Flagg-Newton, J.L., Dahl, G., Loewenstein, W.R. 1981. Cell junction and cyclic-AMP. 1. Upregulation of junctional membrane permeability and junctional membrane particles by administration of cyclic nucleotide or phosphodiesterase inhibitor. *J. Membrane Biol* **63:**105–121

Flagg-Newton, J.L., Loewenstein, W.R. 1981. Cell junction and cyclic AMP. II. Modulation of junctional membrane permeability, dependent on serum and cell density. *J. Membrane Biol.* **63:**123–131

Girsch, S.J., Peracchia, C. 1982. Calcium-activated calmodulin induces conformational changes in lens gap junction protein. *J. Cell Biol.* **95:**103*a*

Girsch, S.J., Peracchia, C. 1983*a*. Lens junction protein changes conformation in the presence of calcium-activated calmodulin. *Invest. Ophthamol. Vis. Sci. Suppl.* **24:**27

Girsch, S.J., Peracchia, C. 1983*b*. Lens junction protein (MIP 26) self-assembles in liposomes forming large channels regulated by calmodulin (CaM). *J. Cell Biol.* **97:**83*a*

Green, D.J., Gillette, R. 1983. Patch and voltage-clamp analysis of cyclic AMP-stimulated inward current underlying neuron bursting. *Nature (London)* **306:**784–785

Hertzberg, E.L., Gilula, N.B. 1981. Liver gap junctions and lens fiber junctions: Comparative analysis and calmodulin interaction. *Cold Spring Harbor Symp. Quant. Biol.* **46:**639–645

Kretsinger, R.H. 1980. Crystallographic studies of calmodulin and homologs. *Ann. N.Y. Acad. Sci.* **356:**14–19

Lees-Miller, J.P., Caveney, S. 1982. Drugs that block calmodulin activity inhibit cell-to-cell coupling in the epidermis of *Tenebrio molitor*. *J. Membrane Biol.* **69:**233–245

Lehrer, S.S., Leavis, P.C. 1974. Fluorescence and conformational changes caused by proton binding to troponin C. *Biochem. Biophys. Res. Commun.* **58:**159–165

Loewenstein, W.R. 1981. Junctional intercellular communication: The cell-to-cell membrane channel. *Physiol. Rev.* **61:**829–913

Obaid, A.L., Socolar, S.J., Rose, B. 1983. Cell-to-cell channels with two independently regulated gates in series: Analysis of junctional conductance modulation by membrane potential, calcium, and pH. *J. Membrane Biol.* **73:**69–89

Peracchia, C. 1980. Structural correlates of gap junction permeation. *Int. Rev. Cytol.* **66:**81–146

Peracchia, C. 1982*a*. Gap junction transport regulation. *In:* Membranes and Transport. A. Martonosi, editor. Vol. 2, pp. 271–278. Plenum, New York

Peracchia, C. 1982*b*. Calmodulin and gap junctions: Reversible inhibition of electrical uncoupling by calmidazolium. *J. Cell Biol.* **95:**102*a*

Peracchia, C. 1984. Cell coupling. *In:* The Enzymes of Biological Membranes. A. Martonosi, editor. Vol. 1, pp. 81–130. Plenum, New York

Peracchia, C., Bernardini, G., Peracchia, L.L. 1981. A calmodulin inhibitor prevents gap junction crystallization and electrical uncoupling. *J. Cell Biol.* **91:**124*a*

Peracchia, C., Bernardini, G., Peracchia, L.L. 1983. Is calmodulin involved in the regulation of gap junction permeability? *Pfluegers Arch.* **399:**152–154

Peracchia, C., Peracchia, L.L. 1980. Gap junction dynamics: Reversible effects of divalent cations. *J. Cell Biol.* **87:**708–718

Rink, T.J., Tsien, R.J., Warner, A.E. 1980. Free calcium in *Xenopus* embryos measured with ion-selective microelectrodes. *Nature (London)* **283:**658–660

Rose, B., Rick, R. 1978. Intracellular pH, intracellular free Ca, and junctional cell-cell coupling. *J. Membrane Biol.* **44:**377–415

Schliwa, M., Euteneuer, V., Bulinski, J.C., Izant, J.G. 1981. Calcium lability of cytoplasmic microtubules and its modulation by microtubule-associated proteins. *Proc. Natl. Acad. Sci. USA* **78:**1037–1041

Siegelbaum, S.A., Camardo, J.S., Kandel, E.R. 1983. Serotonin and cyclic AMP close single K^+ channels in *Aplysia* sensory neurones. *Nature (London)* **299:**413–416

Socolar, S.J., Loewenstein, W.R. 1979. Methods for studying transmission through permeable cell-to-cell junctions. *In:* Methods in Membrane Biology. Vol. 10, pp. 123–179. E.D. Korn, editor. Plenum, New York

Spray, D.C., Harris, A.L., Bennett, M.V.L. 1981*a*. Gap junctional conductance is a simple and sensitive function of intracellular pH. *Science* **211:**712–715

Spray, D.C., Harris, A.L., Bennett, M.V.L. 1981*b*. Glutaraldehyde differentially affects gap junctional conductance and its pH and voltage dependence. *Biophys. J.* **33:**108*a*

Spray, D.C., Stern, J.H., Harris, A.L., Bennett, M.V.L. 1982. Gap junctional conductance: Comparison of sensitivities to H and Ca ions. *Proc. Natl. Acad. Sci. USA* **79:**441–445

Steiner, R.F., Lamboy, P.K., Sternberg, H. 1983. The dependence of molecular dynamics of calmodulin upon pH and ionic strength. *Arch. Biochem. Biophys.* **222:**158–169

Teranishi, T., Negishi, K., Kato, S. 1983. Dopamine modulates S-potential amplitude and dye-coupling between external horizontal cells in calf retina. *Nature (London)* **301:**243–246

Turin, L., Warner, A.E. 1977. Carbon dioxide reversibly abolishes ionic communication between cells of early amphibian embryo. *Nature (London)* **270:**56–57

Turin, L., Warner, A.E. 1980. Intracellular pH in early *Xenopus* embryos: Its effect on current flow between blastomeres. *J. Physiol. (London)* **300:**489–504

Unwin, P.N.T., Ennis, P.D. 1983. Calcium-mediated changes in gap junction structure: Evidence from low angle X-ray pattern. *J. Cell Biol.* **97:**1459–1466

Van Belle, H. 1981. R24571: a potent inhibitor of calmodulin-activated enzymes. *Cell Calcium* **2:**483–494

Weiss, B., Fertel, R., Figlin, R., Uzonov, P. 1974. Selective alteration of the activity of the multiple forms of adenosine 3′, 5′-monophosphate phosphodiesterase of rat cerebrum. *Mol. Pharmacol.* **10:**615–625

Welsh, M.J., Aster, J., Ireland, M., Alcala, J., Maisel, H. 1981. Calmodulin and gap junctions: Localization of calmodulin and calmodulin binding sites in chick lens cells. *J. Cell Biol.* **91:**123*a*

Welsh, M.J., Aster, J.C., Ireland, M., Alcala, J., Maisel, H. 1982. Calmodulin bindings to chick lens gap junction protein in a calcium-independent manner. *Science* **216:**642–644

Welsh, M.J., Dedman, J.R., Brinkley, B.R., Means, A.R. 1978. Calcium-dependent regulator protein: Localization in mitotic apparatus of eukaryotic cells. *Proc. Natl. Acad. Sci. USA* **75:**1867–1871

Welsh, M.J., Dedman, J.R., Brinkley, B.R., Means, A.R. 1979. Tubulin and calmodulin: Effects of microtubule and microfilament inhibitors on localization in the mitotic apparatus. *J. Cell Biol.* **81:**624–634

Wojtczak, J. 1982. Influence of cyclic nucleotides on the internal longitudinal resistance and contractures in the normal and hypoxic mammalian cardiac muscle. *J. Mol. Cell Cardiol.* **14:**259–265

Received 28 November 1983; revised 24 February 1984